REVISION MS # DB19-1043

SUPPLEMENTAL MATERIAL

Flow cytometry and sorting experiments: peripheral blood was collected by submandibular bleeding into EDTA tubes. Ten µL were designated for counting live WBC with a hemocytometer. The remaining blood was designated for fluorescence-activated cell sorting (FACS) and was sequentially (i) subjected to red blood cell lysis, (ii) incubated with anti-mouse FcγRII/III (2.4G2) and a viability dye (Zombie UV); and (iii) stained with the following anti-mouse antibodies (purchased from BioLegend unless noted otherwise): Alexa700-coupled CD45 (clone 30-F11); APC-coupled CD11b (clone M1/70); PE-coupled CD3 (clone 145-2C11), CD19 (clone eBio1D3, eBioscience), and NK1.1 (clone PK136); BV785-coupled Ly6G (clone 1A8); BV605-coupled CD115 (clone AFS98, eBioscience); FITC-coupled Ly6C (clone AL-21, BD Bioscience). PMo were identified and enumerated as $CD45^{hi}/CD11b^{hi}/Lin(CD3/CD19.9/NK1.1)^{neg}/Ly\text{-}6G^{neg}/CD115^{hi}/Ly\text{-}6C^{neg}$, and sorted with a FACSAria II (BD Biosciences, Franklin Lakes, NJ, USA).

In order to identify PMo in the immunohistochemistry experiments we needed a positive marker of PMo. We tested the specificity of the antibody to the activating IgG Fc receptor called FCγgamma RIV (also named CD16.2) in flow cytometry experiments using an APC-coupled CD16.2 antibody (clone 9E9, BioLegend). For these experiments, the antibody panel was modified by substituting the APC-coupled CD11b with BV421-coupled CD11b (clone M1/70).

Intracardiac perfusion and quantitation of leukostasis: we introduced in the experimental protocol derived from published procedures (1) a system of checkpoints to determine the technical adequacy of each experiment. Specific checkpoints monitored during each procedure were: (i) duration of the individual phases of

perfusion (each phase was timed to last 33”, the complete procedure lasted 1’39”), (ii) time to blanching of the liver (less than 4”), (iii) absence of visible lung edema, and (iv) absence of blood at enucleation of the eyes. Only procedures fulfilling these requirements were considered technically successful, and their results included in computation.

Immunohistochemistry: details of the procedure were as follows. Whole retinas were placed in 300 µl of blocking buffer (10% Donkey serum for anti CD45 or 10% Goat serum for anti CD16.2; 1% BSA; 1% Triton X-100; in 1x PBS) for 2 hours at room temperature. The whole retinas were then incubated with the primary antibody Rat anti-mouse CD45 (clone 30-F11; 1:200) or Armenian Hamster anti-mouse CD16.2 (clone 9E9; 1:50) in 300 µl of blocking buffer at 4^{o}C overnight. After washes in 1 ml 1% Triton-X PBS (1% PBST) at room temperature for 30 minutes, the retinas were incubated with Cy3-coupled secondary antibody Donkey anti-Rat (1:400) or Cy3-coupled Goat anti-Armenian Hamster (1:400) in 300 µl of blocking buffer at room temperature for 1 hour. The retinas were washed in 1 ml of the following wash buffers (sequentially): 1% PBST for 30 minutes; 0.5% PBST for 30 minutes X 2; 0.25% PBST for 30 minutes X 2; PBS for 15 minutes. Finally, the retinas were mounted vitreous side up on a glass slide with 5ul of DAPI mounting medium.

Fluorescein Angiography: Mice were anesthetized with an intraperitoneal injection of a Ketamine and Xylazine solution; pupils were dilated with 1% Tropicamide. Baseline fundus images were obtained using a Micron III Retinal Imaging Microscope. Subsequently, 2% Fluorescein was administered intraperitoneally (5uL/g body weight) and images of the retinal vasculature were captured for 8 minutes.

Acellular Capillaries: preparation of retinal trypsin digests and counting of acellular capillaries followed procedures routinely used in our laboratory (2; 3). The eyes were immediately enucleated after sacrifice and fixed in 10% formalin for 48 hours, then washed in glycine overnight. The retinas were dissected and the neural elements

digested with 3% trypsin (Difco Trypsin 250; Difco Laboratories, Detroit, MI, USA) to yield the intact microvascular network. The vascular network was stained with periodic acid Schiff-hematoxylin and examined at 20X magnification using the AxioVision4 program (Carl Zeiss, Germany). Acellular capillaries were defined on the basis of specific characteristics of length and diameter (absence of cell nuclei along segments that were at least 40 μm in length and of a width equal to at least 20% of an average capillary), and their count expressed as number of acellular capillaries per mm^2 retina. The counts reported represent the mean of counts from 3 independent observes performed on masked slides; values beyond 2SD were excluded from the computation.

Supplemental Figure 1

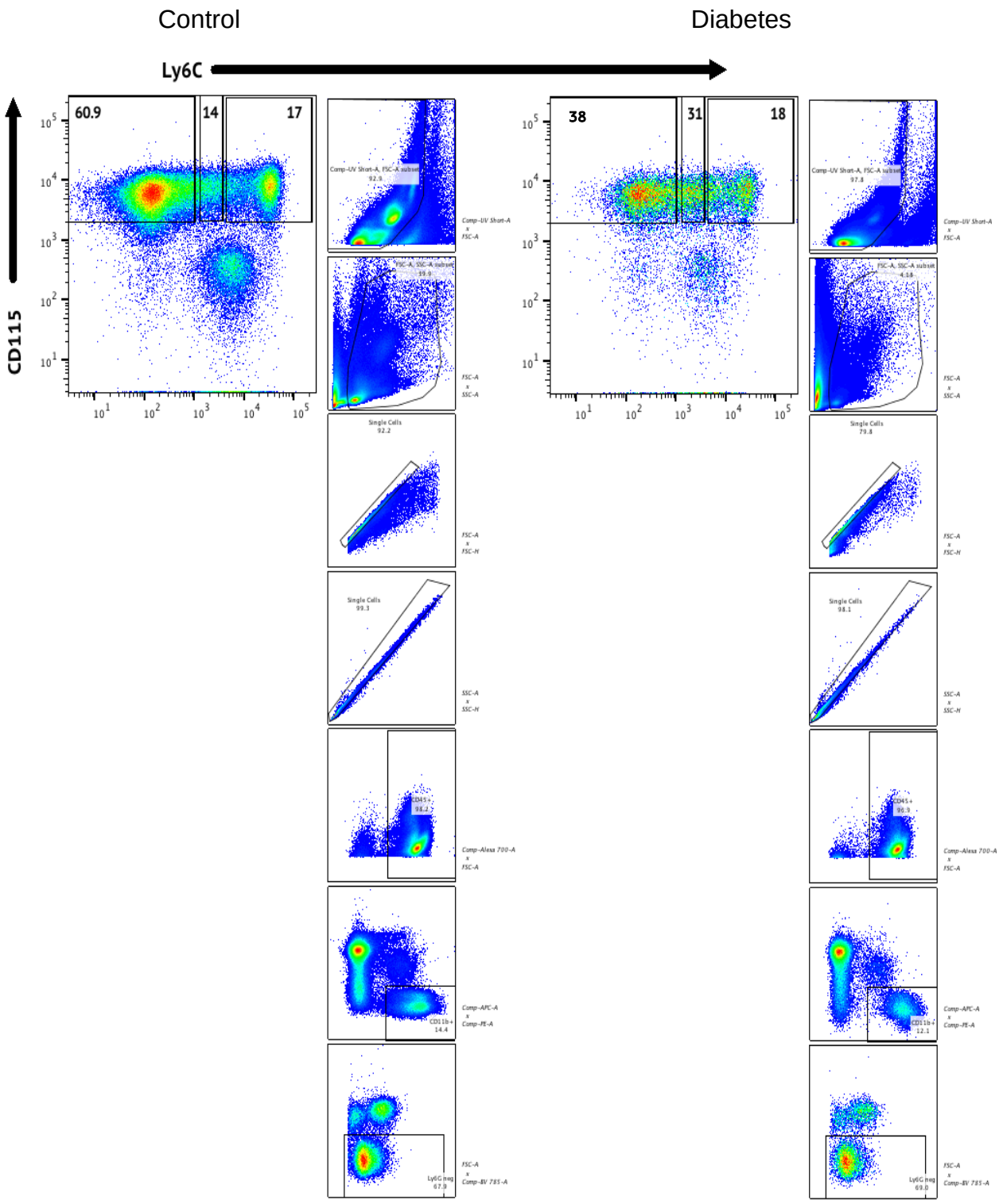

Supplemental Figure 1. Representation of flowcytometry experiments describing the sequential gating strategy used to identify patrolling monocytes, and showing the rearrangement of circulating monocyte subpopulations induced by diabetes. The percentages of Ly6C^{-} (patrolling), Ly6C^{int} (intermediate), and Ly6C^{+} (inflammatory) monocytes were determined from all live CD45^{+}CD11b^{+}Lin^{-}Ly6G^{-}CD115^{+} cells, in WT-Control (left panel) and in WT-diabetic mice (right panel).

Supplemental Figure 2

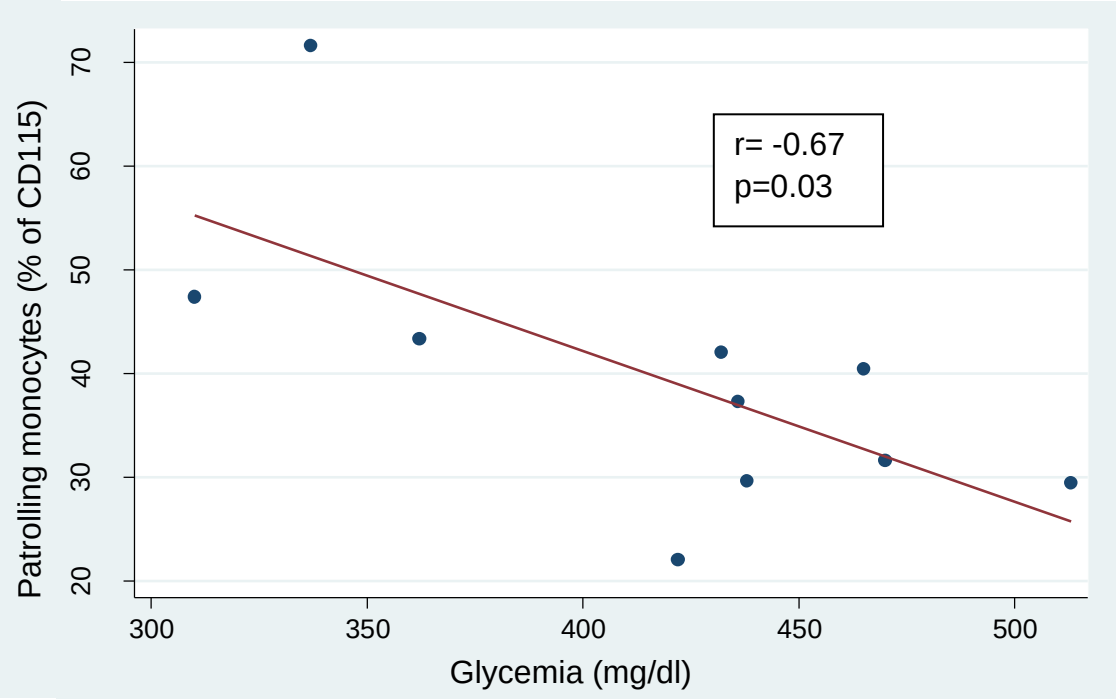

Supplemental Figure 2. Scatterplot of inverse correlation between the number of circulating patrolling monocytes and levels of hyperglycemia in WT-diabetic mice, analyzed by Pearson correlation. The levels of hyperglycemia show a strong inverse correlation with the percentage of circulating patrolling monocytes (r= -0.67, p=0.03). Each point represents an individual mouse. r=Pearson correlation coefficient

Supplemental Figure 3

A.

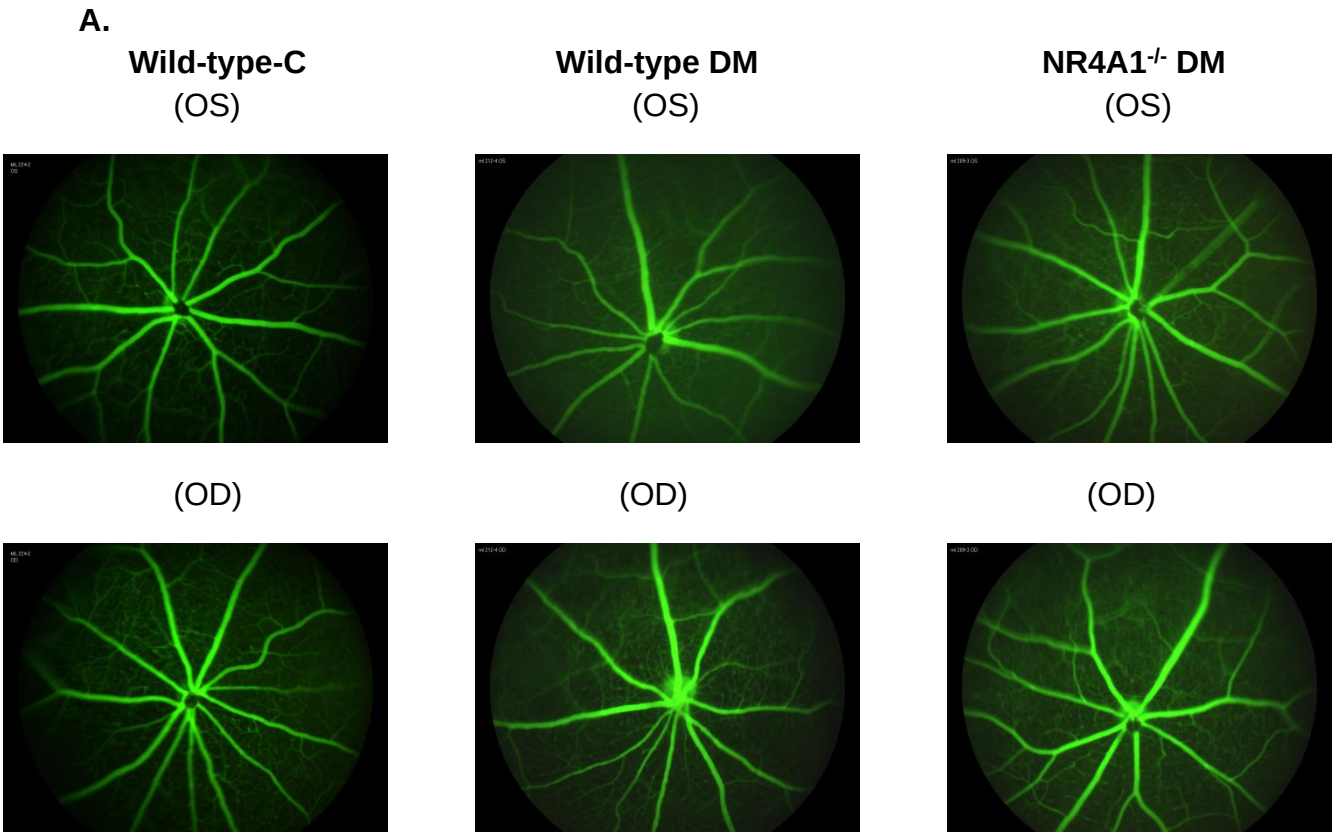

B.

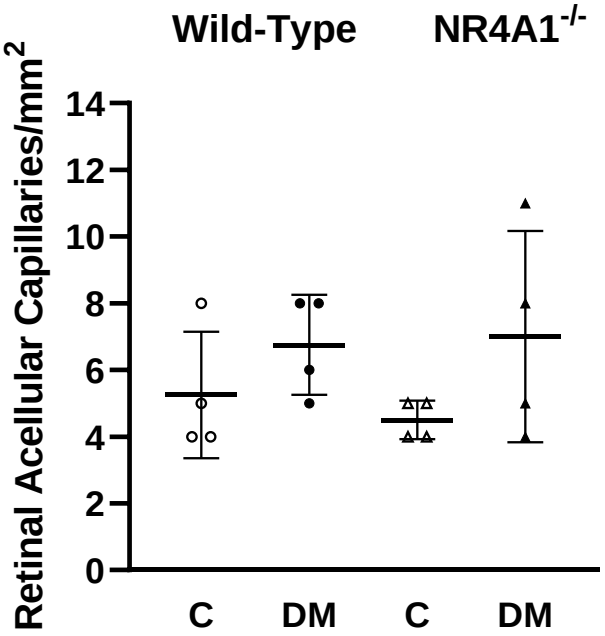

Supplemental Figure 3. Retinal microvessels at 4 months of diabetes.

A. Representative retinal fluorescein angiograms in one wild-type control mice, and one wild-type and one NR4A1-/- mouse at 4 months of diabetes. The angiograms did not show visible alterations of retinal microvessels or leakage. C, control; DM, diabetes; OS, left eye; OD, right eye.

B. The absence of Patrolling monocytes did not cause an increase in microvascular disease in the retina of mice at 4 months of diabetes. Enumeration of retinal acellular capillaries per mm^2 was performed on retinal trypsin digests in wild-type and $NR4A1^{-/-}$ mice at 4 months of diabetes. n=4 mice per group. Scatterplots represent mean±SD. C, control mice; DM, diabetic mice. Statistical analysis was performed using ANOVA for the 4 groups, followed by post-hoc testing with the Bonferroni test.

Supplemental Figure 4

A.

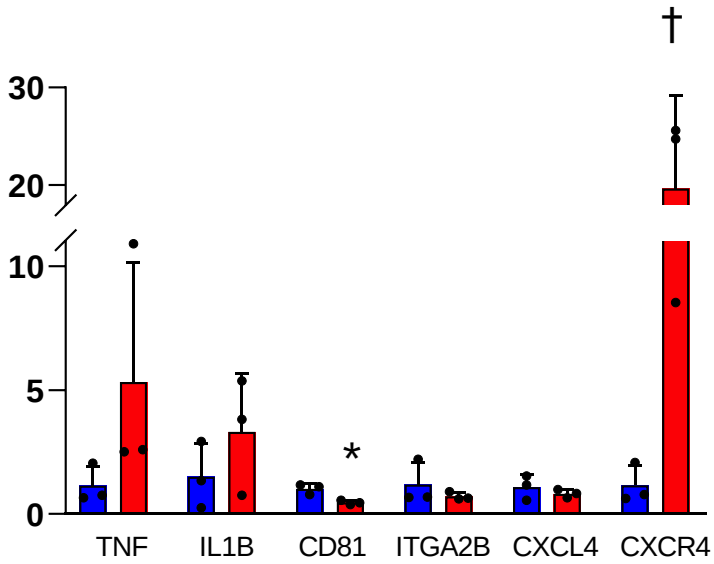

B.

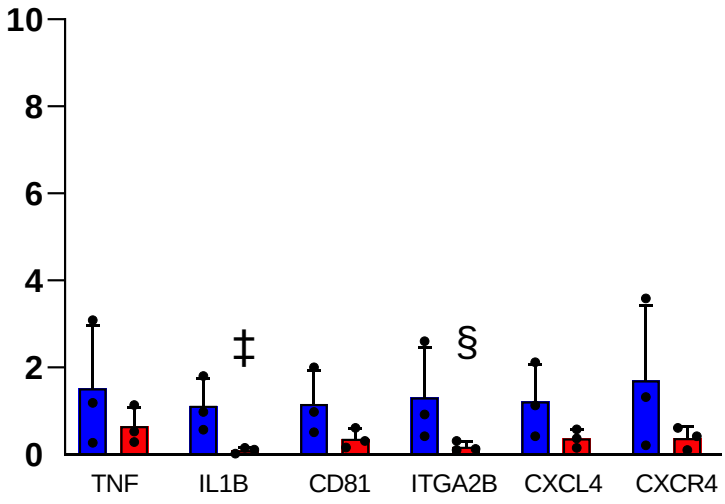

Supplemental Figure 4.

Expression level measured by qPCR of genes selected from the differentially expressed genes between diabetic and control PMo identified by RNAsequencing. Measurements were performed in circulating PMo from wild type mice after short (3 months, panel A), and long (7 months, panel B) duration of diabetes, to be compared with results obtained by RNA sequencing at 5 months of diabetes. (see Supplemental Table 2 for the

characteristics of the experimental mice used for RNA experiments). The gene products tested were TNF-α and IL-1ß, as representative of inflammation; CD81, a facilitator of leukocyte adhesion to vascular endothelium; ITGA2B as representative of the integrin cell adhesion receptor; CXCL4 a secreted angiostatic protein that blocks VEGF and its signaling; and CXCR4 as representative of migration and chemotaxis. The PMo gene expression pattern in mice with 7 months of diabetes duplicated the pattern shown by RNA sequencing at 5 months of diabetes except for pro-migratory CXCR4 that did not show upregulation. CXCR4 upregulation was instead very prominent at 3 months of diabetes, when other gene expression changes were not yet evident. The time-dependent changes in CXCR4 expression, contrasted with the time-course of morphological signs of clinical retinopathy (Figures 4B and C, and Supplemental Figure 3B), suggest that CXCR4 may play a role in delivering the protective activities of patrolling monocytes to the retinal vessels. Bars and scatterplots represent mean±SD. Controls, blue bars; Diabetes, red bars. * $p<0.01$; † $p=0.005$; ‡ $p<0.02$; § $p<0.05$ vs. controls. Statistical analysis was performed using Student *t* test.

Supplemental Table 1

A. Flowcytometry

	n	Age at sacrifice (months)	Body weight at sacrifice (g)	Diabetes Duration (months)	Average Blood Glucose (mg/dl)	Blood Glucose at sacrifice (mg/dl)	HbA1c at sacrifice (%)	HbA1c at sacrifice (mmol/mol)
WT - C	11	7.1±1.8	31±1	-	-	83±15	4.8±0.4	30±4
WT - DM	11	6.9±1.7	25±2*	5.1±1.3	485±78	419±64†	12.3±1.9 †	112±20

B. Intracardiac perfusion/Leukostasis

	n	Age at sacrifice (months)	Body weight at sacrifice (g)	Diabetes Duration (months)	Average Blood Glucose (mg/dl)	Blood Glucose at sacrifice (mg/dl)	HbA1c at sacrifice (%)	HbA1c at sacrifice (mmol/mol)
WT – C	15	5.0±1.7	31±3	-	135±15	124±37	4.6±0.3	27±4
WT - DM	9	5.5 ±1.2	23±2‡	2.7±0.8	544±39‡	495±87‡	11.4±1.6 ‡	107±12
Nr4a1$^{-/-}$ - C	6	5.0±1.7	33±5	-	151±13	138±24	4.3±0.2	24±2
Nr4a1$^{-/-}$ - DM	5	5.7±2.0	22±3‡	3.2±1.0	544±60‡	524±152‡	11.8±1.4 ‡	107±12

C. Microangiopathy at 4 months of diabetes

	n	Age (months)	Body weight (g)	Diabetes Duration (months)	Blood Glucose at sacrifice (mg/dl)	HbA1c at sacrifice (%)	HbA1c at sacrifice (mmol/mol)
WT- C	4	5.0 ± 0.7	34 ± 1	-	130 ± 19	4.4 ± 0.1	20±1
WT- DM	4	5.3± 0.2	25 ± 1§	3.7±0.1	492 ± 76#	11.9 ± 1.2 #	103±13
Nr4a1$^{-/-}$- C	4	5.8 ± 0.5	36 ± 7	-	105 ± 20	4.5 ± 0.4	22±5
Nr4a1$^{-/-}$- DM	4	5.5 ± 0.5	27 ± 3‖	3.7±0.1	424 ± 116#	11.1 ± 1.7 #	94±18

D. Microangiopathy at 6 months of diabetes

	n	Age (months)	Body weight (g)	Diabetes Duration (months)	Blood Glucose at sacrifice (mg/dl)	HbA1c at sacrifice (%)	HbA1c at sacrifice (mmol/mol)
WT- C	19	9.6 ± 3.9	39 ± 7	-	111 ± 18	4.5 ± 0.5	26±6
WT- DM	6	7.3 ± 0.5	27 ± 1**	5.5±0.5	554 ± 80**	12.2 ± 0.7 **	110±8
Nr4a1$^{-/-}$- C	22	9.7 ± 3.5	38 ± 6	-	103 ± 28	4.5 ± 0.4	26±4
Nr4a1$^{-/-}$- DM	10	7.7 ± 0.5	26 ± 2**	5.4±0.4	556 ± 93**	12.5 ± 1.0 **	113±11

Supplemental Table 1. Characteristics of experimental mice used for the indicated types of experiments. **A.** Flowcytometry. Average blood glucose is the mean±SD of weekly blood glucose measurements. *P<0.05 vs. WT-C; †P<0.0001 vs. WT-C. **B.**

Intracardiac perfusion/leukostasis. Average blood glucose is the mean±SD of weekly blood glucose measurements. ‡P=0.0001 vs. WT-C and Nr4a1$^{-/-}$-C. **C.** Microangiopathy at 4 months of diabetes. §P=0.05 vs. WT-C; ||P<0.05 vs. Nr4a1$^{-/-}$-C; #P<0.0001 vs. Nr4a1$^{-/-}$-C and WT-C. **D.** Microangiopathy at 6 months of diabetes. **P<0.0001 vs. WT-C and Nr4a1$^{-/-}$-C. WT, wild-type; C, control mice; DM, diabetic mice. Data are means±SD. Statistical analysis was performed with ANOVA followed by Bonferroni's correction test.

Supplemental Table 2.

Group	n	Age at sacrifice (months)	Body weight at sacrifice (g)	Diabetes Duration (months)	Average Blood Glucose throughout experiment	Blood Glucose at sacrifice (mg/dl)	HbA1c at sacrifice (%)	HbA1c at sacrifice (mmol/mol)	RIN
C-S	3	6.3±1.0	31±1			90±11	5.2±0.2	31±5	9.0±0.3
DM-S	3	5.0±0.0*	26±1	2.7±0.2*	436±89	324±19§	10.1±1.3 **	90±11	8.2±2.1
C-I	3	7.3±0.6	34±7			94±10	4.8±0.4	29±4	9.8±0.2
DM-I	3	7.0±0.0†	24±2	4.8±0.0†	540±61	441±25‖	12.6±0.6 ††	113±7	9.1±0.8
C-L	3	7.1±0.1	31±1			91±8	5.0±0.3	29±6	9.4±0.5
DM-L	3	9.3±0.1‡	26±4	7.0±0.0‡	528±42	446±16#	14.6±0.4 ‡‡	136±4	8.7±0.6

Supplemental Table 2. Characteristics of the WT mice used for the RNA experiments. C-S: controls short duration; DM-S: short duration of diabetes; C-I: controls intermediate duration; DM-I: intermediate duration of diabetes; C-L: controls long duration; DM-L: long duration of diabetes. RIN: RNA integrity number. C and DM mice with intermediate duration of diabetes represent the mice studied in the RNA sequencing experiments. C and DM mice with short and long duration of diabetes represent the mice studied in the qPCR experiments. *P<0.0001 vs DM-I and DM-L; †P<0.0001 vs DM-S and DM-L; ‡P<0.0001 vs DM-S, DM-I, and C-L; §P<0.05 vs C-S; ||P=0.0005 vs C-I; #P<0.0001 vs C-L; **P<0.005 vs C-S; ††P=0.0001 vs C-I; ‡‡P<0.05 vs D-S and D-I. Statistical analysis was performed with Student's *t* test when comparing two groups, and by ANOVA followed by Bonferroni's correction test when comparing three groups.

Supplemental Table 3.

Genes down-regulated by diabetes in Patrolling monocytes				
Gene	**LogFc**	**FC**	**FDR**	**Notes**
INFLAMMATION				
Tnf	-1.47	-2.8	0.0012	Pro-inflammatory
Il1B	-1.022	-2.0	0.0019	Pro-inflammatory
Cd40	-1.19	-2.3	0.022	TNF receptor
Cd6	-8.58	-382.7	0.009	Mediates ischemia/reperfusion injury; CD6-/- mice were protected from intestinal inflammation and mucosal damage in I/R models. CD6 binds to ALCAM on leukocytes (mainly CD19 lymphocytes) and activates them.
Cd28	-7.96	-249.0	0.043	Is expressed in monocytes where it induces the secretion of TNFalfa, IL4, IL2, IL10; Pro apoptotic.
Ppbp	-2.78	-6.9	4.0E-05	Is a potent chemoattractant and activator of neutrophils. Also known as *CXCL7*.
Prkcq	-5.35	-40.8	0.028	Encodes PKC-θ. Pro inflammatory; increases the expression of IFN-γ, IL-2, IL-4, TNF-alfa, IL-6, IL-17. Treatment with PKC-θ inhibitor: (i) preserves tight junction integrity, (ii) reduces chemotaxis, and (iii) reduces inflammation.
Egr1	-3.11	-8.6	0.0037	Transcription factor: acts as a positive regulator of chemokine biosynthesis. Increased expression during hypoxia. Pro-apoptotic (via p53), pro-inflammatory (IL-1b) and pro-atherosclerotic.
Clec4n	-1.99	-4.0	0.041	Is a membrane receptor; when stimulated initiates signaling that leads to the induction of cytokines. Also known as *Dectin-2*.
Niacr1	-9.38	-666.3	8.0E-05	Pro-apoptotic. Encodes GPR109a that increases the secretion of PGE2 (vascular permeability) and PGD2. Its expression is induced by IFNγ. It is the receptor for nicotinic acid (lipid lowering effect) and responsible for the flushing side effect of this molecule. Shown also to possess anti-inflammatory effects.
Ache	-8.76	-433.5	0.0023	Acetylcholinesterase (catalyzes breakdown of Acetylcholine). Its suppression is anti-apoptotic and anti-inflammatory (by increase in acetylcholine levels)
Nanos1	-5.52	-45.9	0.029	Nanos homolog 1. Expressed in macrophages derived from monocytes (more from CD16+ than CD14+). Nanos1 interferes with E-cadherin (reduces its pro-adhesive functions). E-cadherin has also anti-inflammatory actions via activating PI3/akt pathway and suppressing NFkB. Nanos1 also up-regulates the production of MMP14.
CXCL4	-2.21	-4.6	0.0036	Also known as *Pf4.* Secreted protein that acts as angiostatic via (1) blocking VEGF and FGF; (2) displacing VEGF and FGF from their

				cognate receptors; (3) increasing CXCR3-B expression on EC; (4) inhibiting pro-angiogenic integrins. CXCL4 slows down re-endothelialization and inhibits intravascular neoangiogenesis. CXCL4 facilitates monocyte differentiation in to pro-inflammatory macrophages, increases lipid uptake, and is pro-atherosclerotic via esterification of ox-LDL in lesional macrophages. CXCL4 upregulates IL4, 5, 13. CXCL4 is chemotactic and activator of neutrophils, and induces adhesion of neutrophils to the endothelium. Finally, CXCL4 is pro-inflammatory, and regulates coagulation.
Ctla2a	-1.34	-2.5	0.0027	Is a secreted protein, its expression is increased by IL4
Clu	-1.49	-2.8	0.0017	Pro inflammatory by inducing NF-kappa-B expression and activity. Promotes apoptosis.
MIGRATION/ADHESION				
Cd81	-1.86	-3.6	2.1E-10	Reduces the expression of LFA-1, therefore the down-regulation of CD81 results in increased levels of LFA-1. The block pf CD81 reduces the transmigration of monocytes, reduces inflammation, and ameliorates autoimmune encephalomyelitis. In addition CD81 mediates tight adhesion of leukocytes to the endothelium (it is associated to VLA4 that binds VCAM1).
Itga2b	-2.36	-5.13	1.0E-09	Integrin expressed also in monocytes. ITGA2B plays a role in cell mobilization and adhesion to extra cellular matrix or to other cells, via mediating attachment to the actin cytoskeleton. Integrins have also a significant role in cell signaling; and can activate protein kinases involved in the regulation of cell growth, division, survival, differentiation, and apoptosis. ITGA2B-/- mice have decreased levels of TGFb and VEGF-A. SNPs associated to diabetic retinopathy. Also known as *Cd41*.
VASCULAR HOMEOSTASIS				
CXCL4	-2.21	-4.6	0.0036	Also known as *Pf4.* Secreted protein that acts as angiostatic via (1) blocking VEGF and FGF; (2) displacing VEGF and FGF from their cognate receptors; (3) increasing CXCR3-B expression on EC; (4) inhibiting pro-angiogenic integrins. CXCL4 slows down re-endothelialization and inhibits intravascular neoangiogenesis. CXCL4 facilitates monocyte differentiation in to pro-inflammatory macrophages, increases lipid uptake, and is pro-atherosclerotic via esterification of ox-LDL in lesional macrophages. CXCL4 upregulates IL4, 5, 13. CXCL4 is chemotactic and activator of neutrophils, and induces adhesion

				of neutrophils to the endothelium. Finally, CXCL4 is pro-inflammatory, and regulates coagulation.
APOPTOSIS				
Niacr1	-9.38	-666.3	8.0E-05	Pro-apoptotic. Encodes GPR109a that increases the secretion of PGE2 (vascular permeability) and PGD2. Its expression is induced by IFNγ. It is the receptor for nicotinic acid (lipid lowering effect) and responsible for the flushing side effect of this molecule. Shown also to possess anti-inflammatory effects.
Ache	-8.76	-433.5	0.0023	Acetylcholinesterase (catalyzes breakdown of Acetylcholine). Its suppression is anti-apoptotic and anti-inflammatory (by increase in acetylcholine levels)
Cd28	-7.96	-249.0	0.043	Is expressed in monocytes where it induces the secretion of TNFalfa, IL4, IL2, IL10. ACHE is also pro apoptotic.
Egr1	-3.11	-8.6	0.0037	Transcription factor: acts as a positive regulator of chemokine biosynthesis. Increased expression during hypoxia. Pro-apoptotic (via p53), pro-inflammatory (IL-1b) and pro-atherosclerotic.
Nab2	-2.46	-5.5	0.035	Transcriptional regulator NGFI-A binding protein 2. Is pro-apoptotic by activating TRAIL (TNF-related apoptosis inducing ligand)
Clu	-1.49	-2.8	0.0017	Proinflammatory by inducing NF-kappa-B expression and activity. Promotes apoptosis.
Apbb1	-1.5	-2.8	0.0027	DNA damage; translocates to the nucleus and induces apoptosis by recruiting other pro-apoptosis factors such as MAPK8/JNK1
Clu	-1.49	-2.8	0.0017	Proinflammatory by inducing NF-kappa-B expression and activity. Promotes apoptosis
Phlda3	-1.25	-2.4	0.015	Pro-apoptotic, Mediates of hypoxia-induced p53-dependent apoptosis also by inhibiting AKT pro-survivor signaling
Cd24a	-1.23	-2.3	0.041	Pro-apoptotic. Also known as *Cd24*.
Ets1	-1.08	2.1	5.0E-05	Role in hematopoietic cell differentiation. PKC is a major regulator of Ets1. Conflicting data on role of Ets1 in apoptosis: Ets1-deficiency increases T-cells apoptosis and overexpression of Ets1 protects VSMCs from undergoing apoptosis (via p21 activation); on the other hand Ets1 is pro-apoptotic via p53, and stimulates expression of pro apoptotic genes (such as bid).
Itga2b	-2.36	-5.13	1.0E-09	Is an integrin expressed also in monocytes. ITGA2B plays a role in cell mobilization and adhesion to extra cellular matrix or to other cells, via mediating attachment to the actin cytoskeleton. Integrins have also a significant role in cell signaling; and can activate protein kinases involved in the regulation of cell growth, division, survival, differentiation, and

				apoptosis. ITGA2B-/- mice have decreased levels of TGFb and VEGF-A. SNPs associated to diabetic retinopathy. Also known as *Cd41*.
Genes up-regulated by diabetes in Patrolling monocytes				
Gene	**LogFc**	**FC**	**FDR**	**Notes**
INFLAMMATION				
Ifit2	2.26	4.79	8.7E-05	Inhibitory effects after infection; inhibits LPS-induced expression of tumor necrosis factor (TNF), interleukin-6 (IL-6) and CXCL2 (also known as MIP2), this effect is mediated post-transcriptionally, possibly by affecting mRNA stability
Eif4e3	1.07	2.10	0.043	Expressed in human peripheral mononuclear cells; inhibits Eif4e1 upregulation by HIF, and that results in increased NFkB. EIF4E3 represses target expression and oncogenic transformation, in direct contrast to EIF4E1, which stimulates these processes. EIF4E3 overexpression decreases expression of VEGF, c-Myc, Cyclin D1, and NBS1
Hp	1.003	2.00	0.0001	Member of the acute phase plasma proteins. It is expressed in monocytes. It reduces the expression of pro-inflammatory cytokines in monocytes. In addition Hp 2-2 genotype (less efficient) is associated with increased risk of CVD and retinopathy in DM patients
MIGRATION/ADHESION				
Cxcr4	1.06	2.08	0.0044	Receptor for CXCL12 (also known as SDF-1). Binding to SDF1 leads to activation of various intracellular pathways that mediate cell survival, proliferation, chemotaxis, migration, and adhesion. Hence, CXCR4 is anti-apoptotic and pro-migratory.
Ppp1r9a	7.04	131.60	0.00018	Encodes Neurabin I, mediator of repair post stroke (by Sigma-1R). NrbI targets PP1 activity to actin-rich structures in cultured cells to promote filopodia and disassemble the stress fiber network.
Cldn1	8.2	294.07	0.015	Expressed in monocytes; its expression is increased by diabetes. Cldn1 activates MMP2 (and MT-MMP1) which increases motility via enhanced response to CXCL12. Cldn1 is also anti-apoptotic. Possibly angiogenic via interaction with MMPs (Claudin 1 interacts direclty with MMPs). Claudin 1 also activates Notch signaling (directly and via MMPs) that is required for generation and formation of PMO; notably, Notch signaling in monocytes reduces IL-8.
Shtn1	2.26	4.79	1.8E-16	Widely expressed: also in dendritic cells (myelo-monocitic lineage). Shootin1 promotes the polarization of migrating neurons. Two isoforms a (only neuronal) and b (also in other

				cells). Shootin1 acts as a clutch molecule to couple actin filaments and cell adhesions, thereby generating the force underlying these processes. Shootin1 accumulates at cell–cell contact sites of some epithelial cells, where it co-localizes with E-cadherin and the actin-binding protein cortactin. Also important is axonal growth.
VASCULAR HOMEOSTASIS				
Angptl4	9.0	512.00	0.028	Expressed in PBMC. It is secreted. Hypoxia increases expression via HIF. Vasculo-protective. Promotes endothelial cell survival. Angptl4-/- mice have higher levels of monocytes and neutrophils. Reduced levels of ANGPTL4 cause increased atherosclerosis and leukocytosis, and decreased leukocyte apoptosis. Protects from ischemia (anti-ischemic effect) by increasing endothelial cell surface, by blocking the breakdown of endothelial cell junctions, and by reducing inflammation via reduction of ICAM on endothelial cells. Consistent reports on its role in inhibiting vascular permeability. Contradictory data on its role in atherosclerosis.
Rcn3	1.41	2.82	0.003	Inhibits several proteins in the endoplasmic and sarcoplasmic reticulum membranes. Increases the activity and the secretion of PACE4 (aka PCSK6) that is anti-apoptotic, and via CORIN activation, which is anti-hypertensive and cardio-protective. Corin deficiency leads to endothelial dysfunction and vascular remodeling.
APOPTOSIS				
Cxcr4	1.06	2.08	0.0044	Receptor for CXCL12 (also known as SDF-1). Binding to SDF1 leads to activation of various intracellular pathways that mediate cell survival, proliferation, chemotaxis, migration, and adhesion. Hence, CXCR4 is anti-apoptotic and pro-migratory.
Cldn1	8.2	294.07	0.015	Expressed in monocytes; its expression is increased by diabetes. Cldn 1 activates MMP2 (and MT-MMP1) which increases motility via enhanced response to CXCL12. Cldn is also anti-apoptotic. Possibly angiogenic via interaction with MMPs (Claudin 1 interacts direclty with MMPs). Claudin 1 also activates Notch signaling (directly and via MMPs) that is required for generation and formation of PMO; notably, Notch signaling in monocytes reduces IL-8.
Ddit4	1.88	3.68	1.4E-11	Plays a role in the response to changes in cellular energy levels, and in cellular stress, including responses to hypoxia and DNA

				damage. It is a HIF-1 target gene. Inhibits mTOR apoptosis.
Rcn3	1.41	2.82	0.0033	Inhibits several proteins in the endoplasmic and sarcoplasmic reticulum membranes. Increases the activity and the secretion of PACE4 (aka PCSK6) that is anti-apoptotic, and via CORIN activation, which is anti-hypertensive and cardio-protective. Corin deficiency leads to endothelial dysfunction and vascular remodeling.

Supplemental Table 3. Differentially expressed genes (DEGs) in circulating patrolling monocytes from diabetic vs. control mice.

DEGs in PMo from three diabetic vs three control wild-type mice studied with RNA sequencing.

Up- and down-regulated DEGs are clustered by gene function. LogFC= Log fold change; FC= Fold change; FDR= False discovery rate.

Supplemental Table 4.

NAME	SIZE	NES	NOM p-val	FDR q-val
PATHWAYS RELATED TO INFLAMMATION				
BIOCARTA_IL17_PATHWAY	8	-2.9	<0.0001	<0.0001
GO_TUMOR_NECROSIS_FACTOR_MEDIATED_SIGNALING_PATHWAY	87	-2.8	<0.0001	0.0003
HALLMARK_IL2_STAT5_SIGNALING	162	-2.8	<0.0001	<0.0001
PID_IL12_2PATHWAY	47	-2.6	<0.0001	0.001
GO_INFLAMMATORY_RESPONSE	257	-2.5	<0.0001	0.002
GO_NIK_NF_KAPPAB_SIGNALING	72	-2.5	<0.0001	0.004
KEGG_CYTOKINE_CYTOKINE RECEPTOR INTERACTION	117	-2.5	<0.0001	0.0003
GO_CYTOKINE_RECEPTOR_ACTIVITY	54	-2.4	<0.0001	<0.0001
GO_REGULATION_OF_INTERFERON_GAMMA_PRODUCTION	61	-2.3	<0.0001	<0.01
GO_POSITIVE_REGULATION_OF_INTERFERON_GAMMA_PRODUCTION	44	-2.1	0.004	0.04
GO_REGULATION_OF_CYTOKINE_SECRETION	89	-2.0	0.008	0.03
HALLMARK_TNFA_SIGNALING_VIA_NFKB	161	-2.0	0.002	0.01
PATHWAYS RELATED TO IMMUNE SYSTEM				
GO_REGULATION_OF_IMMUNE_RESPONSE	553	-3.2	<0.0001	<0.0001
GO_REGULATION_OF_IMMUNE_SYSTEM_PROCESS	883	-3.1	<0.0001	6.17E-05
REACTOME_ADAPTIVE_IMMUNE_SYSTEM	417	-3.0	<0.0001	<0.0001
GO_ACTIVATION_OF_IMMUNE_RESPONSE	295	-2.9	<0.0001	1.82E-04
REACTOME_IMMUNE_SYSTEM	679	-2.7	<0.0001	5.33E-04
REACTOME_ACTIVATION_OF_NF_KAPPAB_IN_B_CELLS	58	-2.6	<0.0001	0.001
GO_REGULATION_OF_INNATE_IMMUNE_RESPONSE	264	-2.4	<0.0001	0.006
GO_LEUKOCYTE_ACTIVATION	305	-2.4	<0.0001	0.004
REACTOME_IMMUNOREGULATORY_INTERACTIONS_BETWEEN_ A_LYMPHOID_AND_A_NON_LYMPHOID_CELL	32	-2.4	0.002	0.003
GO_ACTIVATION_OF_INNATE_IMMUNE_RESPONSE	170	-2.3	<0.0001	0.01
GO_INNATE_IMMUNE_RESPONSE_ACTIVATING_CELL_SURFACE_ RECEPTOR_SIGNALING_PATHWAY	89	-2.2	<0.0001	0.02
REACTOME_INNATE_IMMUNE_SYSTEM	174	-2.1	<0.0001	0.03
GO_LYMPHOCYTE_ACTIVATION	256	-2.1	<0.0001	0.02
PATHWAYS RELATED TO APOPTOSIS				
REACTOME_REGULATION_OF_APOPTOSIS	50	-2.8	<0.0001	1.77E-04
BIOCARTA_TCAPOPTOSIS_PATHWAY	7	-2.7	<0.0001	5.43E-04
GO_CELL_DEATH	709	-2.4	0.004	0.005985
GO_REGULATION_OF_RESPONSE_TO_STRESS	991	-2.4	<0.0001	0.009816
REACTOME_PD1_SIGNALING	10	-2.2	0.002	0.010305
HALLMARK_APOPTOSIS	125	-2.1	<0.0001	0.008627
PATHWAYS RELATED TO COAGULATION				
GO_PLATELET_DEGRANULATION	66	-2.9	<0.0001	2.79E-04
REACTOME_FORMATION_OF_FIBRIN_CLOT_CLOTTING_CASCADE	17	-2.7	<0.0001	0.0006
HALLMARK_COAGULATION	75	-2.3	0.002	0.003
REACTOME_INTRINSIC_PATHWAY	9	-2.3	0.004	0.008
GO_BLOOD_COAGULATION_INTRINSIC_PATHWAY	9	-2.2	0.002	0.02
REACTOME_PLATELET_ACTIVATION_SIGNALING_AND_AGGREGATION	141	-2.2	<0.0001	0.01
KEGG_COMPLEMENT_AND_COAGULATION_CASCADES	26	+2.0	0.004	0.03

Supplemental Table 4. Gene Set Enrichment analysis (GSEA). Selected pathways enriched in patrolling monocytes are clustered by function. NES, normalized enrichment score. FDR, false discovery rate.

SUPPORTING REFERENCES

1. Rojas M, Zhang W, Xu Z, Lemtalsi T, Chandler P, Toque HA, Caldwell RW, Caldwell RB: Requirement of NOX2 expression in both retina and bone marrow for diabetes-induced retinal vascular injury. PloS one 2013;8:e84357

2. Mizutani M, Kern TS, Lorenzi M: Accelerated death of retinal microvascular cells in human and experimental diabetic retinopathy. J Clin Invest 1996;97:2883-2890

3. Dagher Z, Park YS, Asnaghi V, Hoehn T, Gerhardinger C, Lorenzi M: Studies of rat and human retinas predict a role for the polyol pathway in human diabetic retinopathy. Diabetes 2004;53:2404-2411